WALAILAK JOURNAL
http://wjst.wu.ac.th Article

Stretched Flow of Casson Fluid with Variable Thermal Conductivity

Tasawar HAYAT, Muhammad FAROOQ[*] and Zahid IQBAL

Department of Mathematics, Quaid-i-Azam University, Islamabad 44000, Pakistan

([*]Corresponding author's e-mail: hfarooq99@yahoo.com)

Received: 24 December 2011, Revised: 18 March 2012, Accepted: 21 February 2013

Abstract

This paper looks at the stagnation point flow of Casson fluid towards a stretching surface. In addition, heat transfer analysis is discussed. The thermal conductivity varies linearly with temperature. Series solutions are first presented and then studied for different parameters of interest in this problem.

Keywords: Casson fluid, stagnation point, variable thermal conductivity, viscous dissipation, stretched surface

Introduction

The boundary layer flow induced by a stretching surface is encountered in several engineering processes. Such flow with heat transfer are important in paper production, enhanced recovery of petroleum resources, packed bed reactors, food processing etc. The stagnation point flows arise in many applications including flows over the tips of rockets, aircrafts, submarines and oil ships. Although numerous studies have been reported for stagnation point flows under various aspects [1-5] but such flow towards a stretching surface was firstly examined by Chiam [6]. He has taken the equal values of stretching and free stream velocities. However, no boundary layer was found in such analysis. Afterward, Mahapatra *et al.* [7] reconsidered this flow problem by choosing different stretching and free-stream velocities. In their study, they ensured the existence of boundary layers. Some more recent representative studies in this direction were presented through the works [8-12].

Non-Newtonian fluids have widespread applications in engineering and industry. Several fluids including polymer solutions, drilling mud, paints, ketchup, shampoo etc do not obey Newton's law of viscosity. The relationship between stress and rate of strain in such fluids is not linear. There is more complexity in the equations of non-Newtonian fluids from different quarters. Various constitutive expressions in view of their diverse properties have been presented. Researchers in the field are looking for the analysis of such fluids in various flow geometries [13-18]. Amongst the various fluid models, there is one which is called Casson fluid [19]. Examples of such fluids include jelly, tomato sauce, honey, soup, concentrated fruit juices etc. With this awareness, the objective of the present investigation is to model the stagnation point flow of Casson fluid over a stretching surface. This paper is organized in the following fashion. Flow description and associated mathematical model are given in section two. Section three consists of series solutions of velocity and temperature by the homotopy analysis method [20-25]. Section four discusses convergence and influence of emerging parameters. The main points are summed up in section five.

Mathematical model

Consider the two-dimensional stagnation point flow of an incompressible Casson fluid over a stretching surface (at $y = 0$). The fluid fills $y > 0$. The heat transfer process is further taken into account when thermal conductivity varies with temperature in a linear manner. The rheological equation of state for the isotropic and incompressible flow of a Casson fluid is

$$\pi_{ij} = \begin{cases} 2\left(\mu_B + \frac{p_y}{\sqrt{2\pi}}\right) e_{ij}, \pi > \pi_c \\ 2\left(\mu_B + \frac{p_y}{\sqrt{2\pi_c}}\right) e_{ij}, \pi < \pi_c \end{cases} \tag{1}$$

In above equation $\pi = e_{ij}e_{ij}$ and e_{ij} is the $(i, j)^{th}$ component of the deformation rate, π is the product of the component of deformation rate with itself, π_c is a critical value of this product based on the non-Newtonian model, μ_B is the plastic dynamic viscosity of the non-Newtonian fluid, and p_y is the yield stress of fluid. Using Eq. (1) and conservation of mass, momentum and energy we have the following boundary layer equations:

$$\frac{\partial u}{\partial x} + \frac{\partial v}{\partial y} = 0, \tag{2}$$

$$u\frac{\partial u}{\partial x} + v\frac{\partial u}{\partial y} = U\frac{\partial U}{\partial x} + \nu\left(1+\frac{1}{\beta}\right)\frac{\partial^2 u}{\partial y^2} \tag{3}$$

$$u\frac{\partial T}{\partial x} + v\frac{\partial T}{\partial y} = \frac{1}{\rho c_p}\frac{\partial}{\partial y}\left(\alpha(T)\frac{\partial T}{\partial y}\right) + \frac{\nu}{c_p}\left(1+\frac{1}{\beta}\right)\left(\frac{\partial u}{\partial y}\right)^2, \tag{4}$$

where the Casson fluid parameter $\beta = \mu_B\sqrt{2\pi_c}/p_y$ and u, v are the velocity components in the x - and y - directions.

The boundary conditions are imposed as

$$u = ax, \quad v = 0, \quad T = T_w \quad \text{at } y = 0, \qquad u \to U = cx, \quad T \to T_\infty \quad \text{as } y \to \infty, \tag{5}$$

where $\alpha(T)$ is the temperature-dependent thermal conductivity, μ is the dynamic viscosity, $U = cx$ is the free stream velocity, T and T_∞ are the fluid and ambient temperatures respectively and T_w is the sheet temperature.

The temperature-dependent thermal conductivity can be written as

$$\alpha(T) = \alpha_\infty\left(1+\varepsilon\frac{T-T_\infty}{\Delta T}\right) \tag{6}$$

in which ε is the small parameter, α_∞ is the thermal conductivity of the fluid far away from the plate and $\Delta T = T_w - T_\infty$. We define the following change of variables

$$u = axf'(\eta), \quad \eta = \sqrt{\frac{a}{\nu}}y, \quad \psi = \sqrt{\nu a}xf(\eta), \tag{7}$$

$$v = -\sqrt{a\nu}f(\eta), \quad \theta(\eta) = \frac{T-T_\infty}{T_w-T_\infty}. \tag{8}$$

Here ψ is the stream function, f is the dimensionless stream function and θ is the dimensionless temperature. Making use of the above variables, the incompressibility condition is automatically satisfied while Eq. (2) - (4) become

$$\left(1+\frac{1}{\beta}\right)f''' + ff'' - (f')^2 + A^2 = 0, \tag{9}$$

$$(1+\varepsilon\theta)\theta'' + \Pr f\theta' + \varepsilon(\theta')^2 + \Pr Ec\left(1+\frac{1}{\beta}\right)(f'')^2 = 0, \tag{10}$$

$$f(0) = 0 \quad f'(0) = 1, \quad \theta(0) = 1, \qquad f'(\infty) = A, \quad \theta(\infty) = 0, \tag{11}$$

where prime denotes the differentiation with respect to η, A is the ratio parameter, Pr is the Prandtl number and Ec is the Eckert number.

$$\Pr = \frac{\nu\rho c_p}{\alpha_\infty}, \quad Ec = \frac{a^2x^2}{c_p(T_w-T_\infty)}, \quad A = \frac{c^2}{a^2}, \tag{12}$$

The local Nusselt number Nu_x is given by

$$Nu_x = \frac{h(x)}{\alpha_\infty}, \tag{13}$$

where the heat transfer coefficients $h(x)$ and $q_w(x)$ are defined as

$$h(x) = \frac{q_w(x)}{T_w-T_\infty}, \quad q_w(x) = -\alpha_\infty\left(\frac{\partial T}{\partial y}\right)_{y=0}, \tag{14}$$

The dimensionless form of the local Nusselt number is

$$(\mathrm{Re}_x)^{-1/2}Nu_x = -\theta'(0), \tag{15}$$

and the skin friction C_f is

$$C_f = \frac{-2\tau_{xy}(0)}{\rho U^2}, \quad \tau_{xy} = \mu(1+1/\beta)\left(\frac{\partial u}{\partial y}\right)_{y=0}, \tag{16}$$

or

$$\mathrm{Re}_x^{1/2} C_f = (1+1/\beta) f''(0). \tag{17}$$

in which $\mathrm{Re}_x = Ux/\nu$ is the local Reynolds number.

Solutions by homotopy analysis method (HAM)

In this section we are interested in finding series solutions for the resulted problems. Hence the initial guesses (f_0, θ_0) and auxiliary linear operators $(\mathrm{L_f}, \mathrm{L_\theta})$ along with their properties can be written as

$$f_0(\eta) = A\eta + (1-A)(1-e^{-\eta}), \quad \theta_0(\eta) = e^{-\eta}, \tag{18}$$

$$L_f(f) = \frac{d^3 f}{d\eta^3} - \frac{df}{d\eta}, \; L_\theta(f) = \frac{d^3 f}{d\eta^3} - f \tag{19}$$

$$L_f[C_1 + C_2\exp(\eta) + C_3\exp(-\eta)] = 0, \tag{20}$$

$$L_\theta[C_4\exp(\eta) + C_5\exp(-\eta)] = 0, \tag{21}$$

in which C_i (i = 1 – 5) are the arbitrary constants. The zeroth and m-th order deformation problems are:

Zeroth order problem

$$(1-p)L_f\left[\hat{f}(\eta;p) - f_0(\eta)\right] = p\hbar_f N_f\left[\hat{f}(\eta;p)\right], \tag{22}$$

$$(1-p)L_\theta[\hat{\theta}(\eta;p) - \theta_0(\eta)] = p\hbar_\theta N_\theta\left[\hat{\theta}(\eta;p), \hat{f}(\eta;p)\right], \tag{23}$$

$$\hat{f}(0;p) = 0, \hat{f}'(0;p) = 1, \hat{f}'(\infty;p) = A, \tag{24}$$

$$\hat{\theta}(0;p) = 1, \; \hat{\theta}(\infty;p) = 0, \tag{25}$$

$$N_f\left[\hat{f}(\eta;p)\right] = \left(1+\frac{1}{\beta}\right)\frac{\partial^3 \hat{f}(\eta;p)}{\partial\eta^3} + \hat{f}(\eta;p)\frac{\partial^2 \hat{f}(\eta;p)}{\partial\eta^2} - \left(\frac{\partial \hat{f}(\eta;p)}{\partial\eta}\right)^2 + A^2, \tag{26}$$

$$N_\theta\left[\hat{\theta}(\eta;p), \hat{f}(\eta;p)\right] =$$
$$\left(1+\epsilon\hat{\theta}(\eta;p)\right)\frac{\partial^2\hat{\theta}(\eta;p)}{\partial\eta^2} + \mathrm{Pr}\hat{f}(\eta;p)\frac{\partial\hat{\theta}(\eta;p)}{\partial\eta} + \epsilon\left(\frac{\partial\hat{\theta}(\eta;p)}{\partial\eta}\right)^2 + PrEc\left(1+\frac{1}{\beta}\right)\left(\frac{\partial^2\hat{f}(\eta;p)}{\partial\eta^2}\right)^2. \tag{27}$$

where $p\in[0,1]$ is the embedding parameter and $\hbar_f$ and $\hbar_\theta$ are the non-zero auxiliary parameters.

***m* th-order deformation problems**

$$L_f[f_m(\eta) - \chi_m f_{m-1}(\eta)] = \hbar_f R_m^f(\eta), \tag{28}$$

$$L_\theta[\theta_m(\eta) - \chi_m \theta_{m-1}(\eta)] = \hbar_\theta R_m^\theta(\eta), \tag{29}$$

$$f_m(0) = f_m'(0) = f_m'(\infty) = f_m''(\infty) = 0, \tag{30}$$

$$\theta_m(0) = \theta_m(\infty) = 0, \tag{31}$$

$$\mathbf{R}_m^f(\eta) = \left(1 + \frac{1}{\beta}\right) f_{m-1}'''(\eta) + \sum_{k=0}^{m-1}\left[f_{m-1-k} f_k'' - f_{m-1-k}' f_k'\right] + A^2(1 - \chi_m), \tag{32}$$

$$\mathbf{R}_m^\theta(\eta) = \theta_{m-1}'' + \varepsilon\sum_{k=0}^{m-1}\theta_{m-1-k}\theta_k'' + \Pr\sum_{k=0}^{m-1}\theta_{m-1-k}' f_k + \varepsilon\sum_{k=0}^{m-1}\theta_{m-1-k}'\theta_k' + \Pr Ec\left(1 + \frac{1}{\beta}\right)\sum_{k=0}^{m-1} f_{m-1-k}'' f_k'', \tag{33}$$

$$\chi_m = \begin{cases} 0, & m \le 1 \\ 1, & m > 1 \end{cases}. \tag{34}$$

For $p = 0$ and $p = 1$, one may write

$$\hat{f}(\eta;0) = f_0(\eta),\ \ \hat{f}(\eta;1) = f(\eta), \tag{35}$$

$$\hat{\theta}(\eta;0) = \theta_0(\eta),\ \ \hat{\theta}(\eta;1) = \theta(\eta) \tag{36}$$

and when p increases from 0 to 1 then $\hat{f}(\eta;p)$ and $\hat{\theta}(\eta;p)$ vary from the initial solutions $f_0(\eta)$ and $\theta_0(\eta)$ to final solutions $f(\eta)$ and $\theta(\eta)$ respectively. Here $\hbar$ is the non-zero auxiliary parameter. By Taylor's theorem and Eq. (35) and (36), we may get

$$\hat{f}(\eta;0) = f_0(\eta) + \textstyle\sum_{m=1}^{\infty} f_m(\eta)p^m,\ \ f_m(\eta) = \frac{1}{m!}\left.\frac{\partial^m f(\eta;p)}{\partial p^m}\right|_{p=0} \tag{37}$$

$$\hat{\theta}(\eta;0) = \theta_0(\eta) + \textstyle\sum_{m=1}^{\infty} \theta_m(\eta)p^m,\ \ \theta_m(\eta) = \frac{1}{m!}\left.\frac{\partial^m \theta(\eta;p)}{\partial p^m}\right|_{p=0} \tag{38}$$

Note that the auxiliary parameters are so properly chosen that the series (37) and (38) converge at $p = 1$ i.e.

$$f(\eta) = f_0(\eta) + \sum_{m=1}^{\infty} f_m(\eta), \tag{39}$$

$$\theta(\eta) = \theta_0(\eta) + \sum_{m=1}^{\infty}\theta_m(\eta). \tag{40}$$

The general solutions (f_m,θ_m) of Eq. (28) and (29) in terms of special solutions $\left(f_m^*, \theta_m^*\right)$ are

$$f_{\mathrm{m}}(\eta) = f_m^*(\eta) + C_1 + C_2 e^{\eta} + C_3 e^{-\eta}, \tag{41}$$

$$\theta_{\mathrm{m}}(\eta) = \theta_m^*(\eta) + C_4 e^{\eta} + C_5 e^{-\eta}, \tag{42}$$

where the constants C_I (I = 1 - 5) through the boundary conditions (30) and (31) have the values

$$C_2 = C_4 = 0, \quad C_3 = \left.\frac{\partial f_m^*(\eta)}{\partial \eta}\right|_{\eta=0}, \quad C_1 = -C_3 - f_m^*(0),$$
$$C_5 = -\theta_m^*(\eta)|_{\eta=0} \tag{43}$$

Analysis of the solutions

It is quite clear that the derived homotopy solutions contain the auxiliary parameters $\hbar_f$ and $\hbar_\theta$. Such parameters are very important in controlling the convergence of series solutions. For appropriate range of auxiliary parameters, we plot the $\hbar$- curves at 15th-order of approximations (**Figures 1** and **2**). These figures show that meaningful values of $\hbar_f$ and $\hbar_\theta$ are $-1.55 \le \hbar_f \le -0.25$ and $-1.0 \le \hbar_\theta \le -0.5$. Also **Table 1** depicts that the series solutions are convergent up to five decimal places.

Figures 3 - 9 show the variations of involved physical parameters on the velocity and temperature. The variation of velocity with respect to Casson parameter is presented in **Figure 3**. This figure depicts that velocity decreases by increasing β. We also note that the increase of parameter β causes a decrease in boundary layer thickness. **Figure 4** shows the effect of ratio parameter A on the velocity profile. Increase in A leads to an increase in velocity profile. **Figure 5** presents the influence of the Eckert number Ec on the temperature. Increasing the value of Ec produces higher temperatures. There is also an increase in the thermal boundary layer thickness when Ec increases. The effect of varying Prandtl number Pr on the temperature profile θ is studied in **Figure 6**. Here an increase in Pr decreases the temperature profile and thermal boundary layer thickness. **Figure 7** depicts the influence of small parameter ε on the temperature. It is seen that an increase in the values of ε produces a higher temperature profile. This **Figure 7** also shows an increase in the thermal boundary layer thickness. Variations in the ratio parameter A and Casson parameter β on the skin friction coefficient are plotted in **Figure 8**. It is observed that by increasing the values of both A and β the skin friction coefficient decreases. Effects of small parameter ε and Eckert number Ec on the Nusselt number are sketched in **Figure 9**. There is a decrease in the Nusselt number when ε and Ec are increased.

The study of **Table 1** indicates that a 13th-order approximation gives a convergent series solution for the velocity profile whereas a 23th-order approximation gives a convergent series solution for the temperature profile.

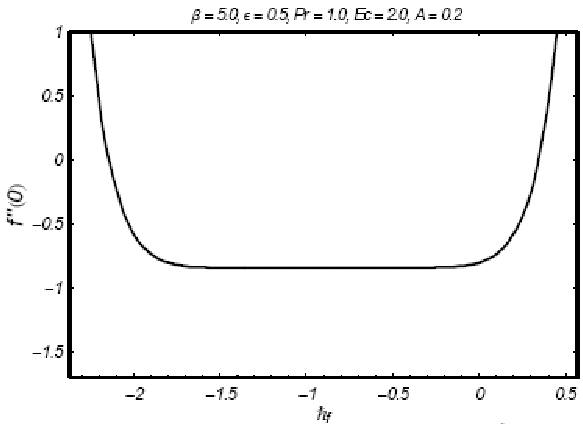

Figure 1 $\hbar$-curve for the function *f*.

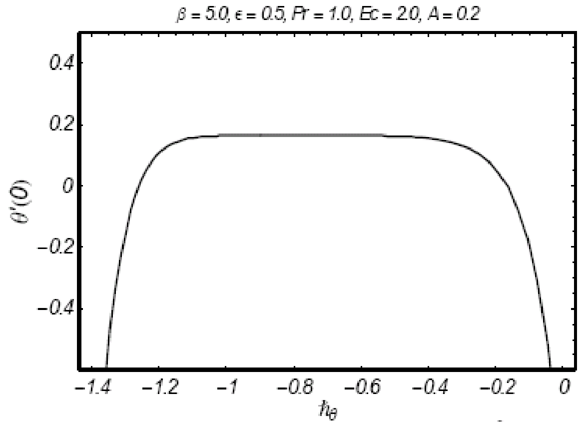

Figure 2 $\hbar$-curve for the function θ.

Table 1 Convergence of the homotopy solutions for different order of approximation when Pr = 1.0, β = 5.0, ε = 0.5, *Ec* = 2.0 and *A* = 0.2.

Order of approximation	$-f''(0)$	$\theta'(0)$
5	0.83578	0.082526
10	0.83803	0.15615
13	0.83811	0.16261
15	0.83811	0.16391
20	0.83811	0.16467
23	0.83811	0.16475
25	0.83811	0.16475
30	0.83811	0.16475

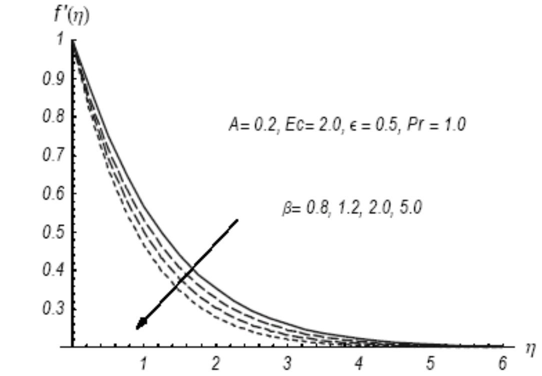

Figure 3 Effect of β on f'.

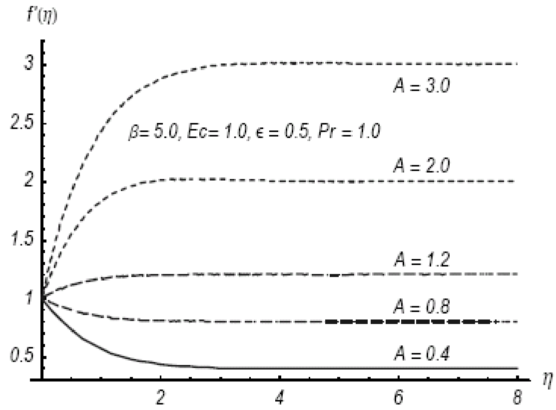

Figure 4 Effect of A on f'.

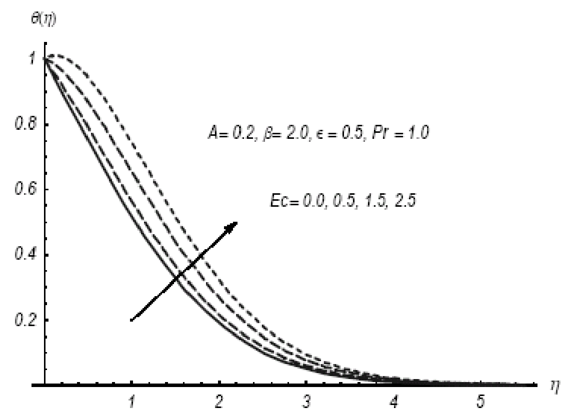

Figure 5 Effect of Ec on θ.

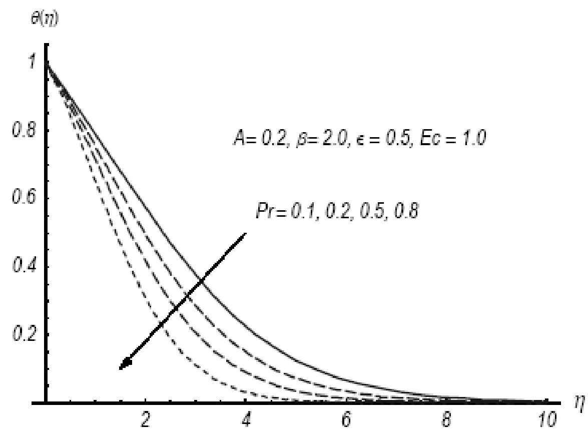

Figure 6 Effect of Pr on θ.

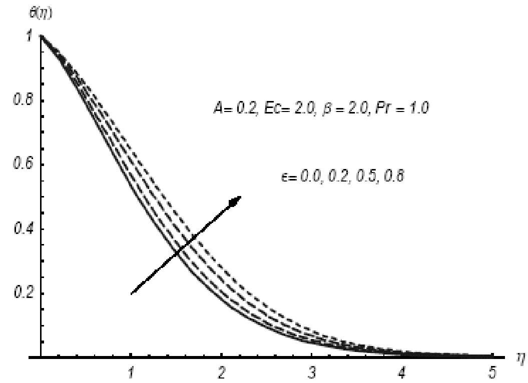

Figure 7 Effect of ϵ on θ.

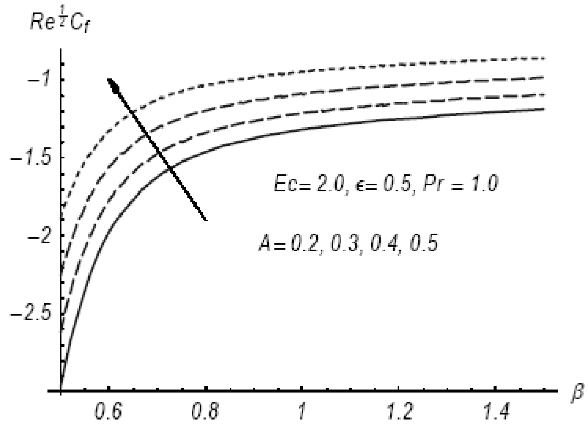

Figure 8 Effects of *A* and β on the skin friction.

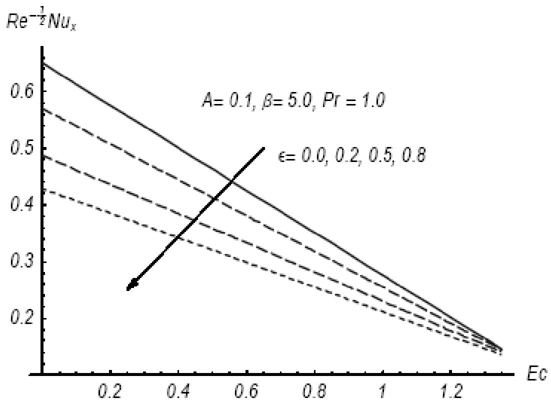

Figure 9 Effects of ϵ and Ec on the Nusselt number.

Main points

In this work, the effect of variable thermal conductivity on the stagnation point flow of Casson fluid is studied. The main observations of this study are as follows.

1. Dimensionless velocity and associated boundary layer thickness are decreasing functions of β.

2. The velocity increases with respect to ratio parameter A.

3. The effects of Ec and Pr on the temperature and thermal boundary layer thickness are opposite.

4. Influence of small parameter ε and Ec on the temperature and thermal boundary layer thickness is similar qualitatively.

5. Skin friction coefficient decreases with the increase in Casson parameter, β.

6. The Nusselt number decreases upon increases in the Eckert number Ec.

References

[1] Y Zhong and T Fang. Unsteady stagnation-point flow over a plate moving along the direction of flow impingement. *Int. J. Heat Mass Trans*. 2011; **54**, 3103-8.

[2] K Bhattacharyya and K Vajravelu. Stagnation-point flow and heat transfer over an exponentially shrinking sheet. *Comm. Nonlinear Sci. Numer. Simulat.* 2012; **17**, 2728-34.

[3] K Bhattacharyya and GC Layek. Effects of suction/blowing on steady boundary layer stagnation-point flow and heat transfer towards a shrinking sheet with thermal radiation. *Int. J. Heat Mass Trans*. 2011; **54**, 302-7.

[4] T Fang, CF Lee and J Zhang. The boundary layers of an unsteady incompressible stagnation-point flow with mass transfer. *Int. J. Nonlinear Mech.* 2011; **46**, 942-8.

[5] T Hayat and M Nawaz. Unsteady stagnation point flow of viscous fluid caused by an impulsively rotating disk. *J. Taiwan Inst. Chemical Eng*. 2011; **42**, 41-9.

[6] TC Chiam. Stagnation-point flow towards a stretching plate. *J. Phys. Soc. Jpn*. 1994; **63**, 2443-4.

[7] TR Mahapatra, SK Nandy and AS Gupta. Magnetohydrodynamic stagnation-point flow of a power-law fluid towards a stretching surface. *Int. J. Nonlinear Mech*. 2009; **44**, 124-9.

[8] S Nadeem, A Hussain and M Khan. HAM solutions for boundary layer flow in the region of the stagnation point towards a stretching sheet. *Comm. Nonlinear Sci. Numer. Simulat*. 2010; **15**, 475-81.

[9] SS Hou, SS Yang and TH Lin. An experimental study on combustion characteristics of flames in a coaxial flow with a stagnation point. *Int. J. Heat Mass Trans*. 2004; **47**, 947-58.

[10] Z Abbas, Y Wang, T Hayat and M Oberlack. Mixed convection in the stagnation-point flow of a Maxwell fluid towards a vertical stretching surface. *Nonlinear Anal. R. World*

Appl. 2010; **11**, 3218-28.

[11] M Mustafa, T Hayat, I Pop, S Asghar and S Obaidat. Stagnation-point flow of a nanofluid towards a stretching sheet. *Int. J. Heat Mass Trans*. 2011; **54**, 5588-94.

[12] M Hassani, MM Tabar, H Nemati, G Domairry and F Noori. An analytical solution for boundary layer flow of a nanofluid past a stretching sheet. *Int. J. Therm. Sci.* 2011; **50**, 2256-63.

[13] M Jamil and C Fetecau. Helical flows of Maxwell fluid between coaxial cylinders with given shear stresses on the boundary. *Nonlinear Anal. R. World Appl.* 2010; **11**, 4302-11.

[14] Y Yao and Y Liu. Some unsteady flows of a second grade fluid over a plane wall. *Nonlinear Anal. R. World Appl.* 2010; **11**, 4442-50.

[15] S Wang and W Tan. Stability analysis of soret-driven double-diffusive convection of Maxwell fluid in a porous medium. *Int. J. Heat Fluid Flow* 2011; **32**, 88-94.

[16] T Hayat, SA Shehzad, M Qasim and S Obaidat. Radiative flow of a Jeffery fluid in porous medium with power law heat flux and heat source. *Nucl. Eng. Des.* 2012; **243**, 15-9.

[17] S Wang and M Xu. Axial couette flow of two kinds of fractional viscoelastic fluids in an Annulus. *Nonlinear Anal. R. World Appl.* 2009; **10**, 1087-96.

[18] C Fetecau, M Mahmood and M Jamil. Exact solutions for the flow of a viscoelastic fluid induced by a circular cylinder subject to a time dependent shear stress. *Comm. Nonlinear Sci. Numer. Simulat*. 2010; **15**, 3931-8.

[19] NTM Eldabe and MGE Salwa. Heat transfer of MHD non-Newtonian Casson fluid flow between two rotating cylinders. *J. Phys. Soc. Japan* 1995; **64**, 41-74.

[20] SJ Liao. Beyond perturbation: introduction to the homotopy analysis method. CRC press LLC, 2004.

[21] S Abbasbandy and T Hayat. On series solution for unsteady boundary layer equations in a special third grade fluid. *Comm. Nonlinear Sci. Numer. Simulat*. 2011; **16**, 3140-6.

[22] MM Rashidi and SAM Pour. Analytic approximate solutions for unsteady boundary-layer flow and heat transfer due to a stretching sheet by homotopy analysis method. *Nonlinear Anal. Model. Contr.* 2010; **15**, 83-95.

[23] T Hayat, M Qasim and Z Abbas. Homotopy solution for unsteady three-dimensional MHD flow and mass transfer in a porous space. *Comm. Nonlinear Sci. Numer. Simulat*. 2010; **15**, 2375-87.

[24] B Yao. Series solution of the temperature distribution in the Falkner-Skan wedge flow by the homotopy analysis method. *Euro. J. Mech. B Fluids*. 2009; **28**, 689-93.

[25] CS Liu. The essence of the homotopy analysis method. *Appl. Math. Comp*. 2010; **216**, 1299-303.